

1 **New insights into the reconstructed temperature in**
2 **Portugal over the last 400-years**

3 **J. A. Santos¹, M. F. Carneiro¹, A. Correia², M. J. Alcoforado³, E. Zorita⁴, J. J.**
4 **Gómez-Navarro⁵**

5 [1] {Centre for the Research and Technology of Agro-Environmental and Biological
6 Sciences, CITAB, Universidade de Trás-os-Montes e Alto Douro, UTAD, 5000-801 Vila
7 Real, Portugal }

8 [2] {Department of Physics and Geophysical Centre of Évora, University of Évora, Évora,
9 Portugal }

10 [3] {Centro de Estudos Geográficos, IGOT, Universidade de Lisboa, Ed. Faculdade de Letras,
11 1600-214 Lisboa, Portugal }

12 [4] {Institute for Coastal Research, Helmholtz-Zentrum Geesthacht, Geesthacht, Germany }

13 [5] {Climate and Environmental Physics, Physics Institute and Oeschger Centre for Climate
14 Change Research, University of Bern, 3012 Bern, Switzerland }

15

16 Correspondence to: J. A. Santos (jsantos@utad.pt);

17

18 **Abstract**

19 The consistency of an existing reconstructed annual (December–November) temperature
20 series for the Lisbon region (Portugal) from 1600 onwards, based on a European-wide
21 reconstruction, with: (1) five local borehole temperature-depth profiles; (2) synthetic
22 temperature-depth profiles, generated from both reconstructed temperatures and two regional
23 paleoclimate simulations in Portugal; (3) instrumental data sources over the twentieth century;
24 and (4) temperature indices from documentary sources during the late Maunder Minimum
25 (1675–1715) is assessed. The low-frequency variability of the reconstructed temperature in
26 Portugal is not entirely consistent with local borehole temperature-depth profiles and with the
27 simulated response of temperature in two regional paleoclimate simulations driven by
28 reconstructions of various climate forcings. Therefore, the existing reconstructed series is
29 calibrated by adjusting its low-frequency variability to the simulations (first-stage
30 adjustment). The annual reconstructed series is then calibrated in its location and scale
31 parameters, using the instrumental series and a linear regression between them (second-stage
32 adjustment). This calibrated series shows clear footprints of the Maunder and Dalton minima,
33 commonly related to changes in solar activity and explosive volcanic eruptions, and a strong
34 recent-past warming, commonly related to human-driven forcing. Lastly, it is also in overall
35 agreement with annual temperature indices over the late Maunder Minimum in Portugal. The
36 series resulting from this post-reconstruction adjustment can be of foremost relevance to
37 improve the current understanding of the driving mechanisms of climate variability in
38 Portugal.

39

40 **Keywords:** Reconstructed temperature, borehole climatology, paleoclimate simulations,
41 historical climatology, non-linear long-term trend, Portugal

42

43 **1. Introduction**

44 Climate reconstructions allow further insight into the climatic variability beyond the relatively
45 short instrumental period, being commonly based on early instrumental records, documentary
46 evidence, namely memoirs, diaries, chronicles, weather logs, ship logbooks, and natural
47 proxies, such as boreholes, tree-rings, corals, ice-cores, speleothem records, pollen-profiles
48 (Brázdil et al., 2010; Brázdil et al., 2005; Camuffo et al., 2010; Li et al., 2010; Luterbacher et
49 al., 2006; Pollack and Huang, 2000). Historical climatology is critical for understanding the
50 driving processes of climate variability not only in the past, but also in the future. This is
51 particularly important when developing climate change projections for the future under
52 emission scenarios (IPCC, 2013).

53 Climate variability in Europe over the last millennium was reconstructed based on both
54 documentary evidence and natural proxies (e.g. Alcoforado et al., 2000; Brázdil et al., 2010;
55 Brázdil et al., 2005; Camuffo et al., 2013; González-Rouco et al., 2009; Luterbacher et al.,
56 2006). European-wide temperature reconstructions since 1500 were already developed
57 (Luterbacher et al., 2004; Xoplaki et al., 2005), as well as continental-wide reconstructions for
58 the last two millennia by Ahmed et al. (2013). Temperature reconstructions in some European
59 sites, based on both documentary data and instrumental records since the 16th century, were
60 carried out by Camuffo et al. (2010). A temperature reconstruction for southern Portugal
61 during the late Maunder Minimum (LMM; 1675-1715) was presented by Alcoforado et al.
62 (2000). However, in Portugal, most of the pre-instrumental records show numerous temporal
63 gaps and there is a substantial lack of natural proxies with clear climatic signals (Alcoforado
64 et al., 2012; Camuffo et al., 2010; Luterbacher et al., 2006).

65 Borehole temperature-depth profiles can be used as paleoclimate proxies for climate
66 reconstruction (e.g. Bodri and Čermák, 1997; González-Rouco et al., 2009; Majorowicz et al.,
67 1999; Šafanda et al., 2007), as they provide independent information on long-term
68 temperature variability (Jones et al., 2009). Borehole measurements are a complementary
69 temperature record to high-frequency air temperature series recorded at weather stations and,
70 through profile inversion methods, may also enable validating low-frequency variability in
71 these series (e.g. Beltrami and Bourlon, 2004; Beltrami and Mareschal, 1995; Beltrami et al.,
72 2011; Chouinard and Mareschal, 2007; González-Rouco et al., 2006; Gouirand et al., 2007;
73 Harris and Chapman, 1998; Harris and Gosnold, 1999; Nielsen and Beck, 1989; Pollack et al.,
74 2006). Some studies have been carried out using borehole temperature logs measured in

75 southern Portugal (e.g. Correia and Šafanda, 2001; Correia and Šafanda, 1999; Šafanda et al.,
76 2007). Borehole reconstructions can also be compared to paleoclimate simulations generated
77 by Earth system models for validation purposes (Beltrami et al., 2006; González-Rouco et al.,
78 2009; Stevens et al., 2008).

79 The present study aims at analysing the consistency between the Luterbacher et al. (2004) and
80 Xoplaki et al. (2005) temperature reconstructions for the Lisbon region (Portugal) and over
81 the period of 1600–1999 using: 1) five local borehole temperature-depth profiles; 2) synthetic
82 temperature-depth profiles, generated from gridded near-surface temperatures produced by
83 regional paleoclimate reconstructions and simulations; 3) instrumental data recorded in
84 Lisbon over the twentieth century; and 4) temperature indices from early instrumental and
85 documentary sources during the LMM (1675-1715). This analysis allows a validation of the
86 annual mean reconstructed temperature in Portugal over the last 400 years. The identification
87 of possible inconsistencies with the above-referred data sources enables a post-reconstruction
88 adjustment of this time series. In effect, this calibrated time series may help understanding
89 past climate variability in Portugal and its main driving mechanisms, namely the role of
90 external vs. internal forcing mechanisms on temperature variability. This attribution analysis
91 provides critical information for model validation and for assessing the reliability of regional
92 climate change projections. The datasets and methods are presented in section 2, the results
93 are discussed in section 3 and the main conclusions are summarized in section 4.

94

95 **2. Data and Methods**

96 **2.1 Reconstructed temperatures**

97 The reconstructed seasonal mean temperature in the gridbox (38.5–39.0°N, 8.0–8.5°W),
98 which is located in the area of Lisbon (Portugal), and for the period of 1600-1999 was
99 extracted from the Luterbacher et al. (2004) and Xoplaki et al. (2005) European-wide
100 reconstructions (Lut2004 henceforth). Data is originally defined on a 0.5° latitude × 0.5°
101 longitude grid. From 1901 onwards this dataset is based on instrumental data from New et al.
102 (2000). For the selected gridbox, it is largely based on temperature records from Lisbon.
103 Since the present study focuses on annual series, annual mean temperatures were obtained by
104 averaging the four values corresponding to winter (DJF), spring (MAM), summer (JJA) and
105 autumn (SON) mean temperatures (no monthly data is available). Hence, annual means refer

106 to the period from December of the previous year to November of that year (e.g. annual mean
107 of 1710 corresponds to the average taken from December 1709 to November 1710).

108

109 **2.2 Borehole data**

110 The consistency of the Lut2004 reconstruction with borehole measurements, retrieved from
111 the only geothermal-paleoclimatological observatory in Portugal (38.34° N; 7.58° W), is
112 assessed. This observatory is located about 5 km northwestwards of Évora (southern Portugal)
113 and about 100 km eastwards of Lisbon. More detailed information can be found in Correia
114 and Šafanda (2001) and Šafanda et al. (2007). Although the borehole measurements were not
115 taken in Lisbon, the variability in the 11-yr moving averages of annual mean temperatures in
116 Évora and Lisbon is quite similar (not shown). In fact, the correlation coefficient is of about
117 0.98 in their common instrumental period (1941-1999). The means for Lisbon and Évora are
118 of 16.8°C and 15.8°C, respectively, while both standard deviations are of ca. 0.3°C. Hence,
119 these borehole measurements are assumed to be representative of the measurements made in
120 Lisbon, as they mostly capture long-term variability.

121 Five measurements (temperature logs) in the same borehole TGQC1 are considered herein,
122 which were carried out on 24 March 1997 (M1), 27 March 2000 (M2), 14 November 2002
123 (M3), 26 November 2003 (M4), and 28 October 2004 (M5), respectively. These five
124 temperature logs were obtained by measuring the equilibrium temperature with a thermistor
125 every 5.0 m (M1), 1.0 m (M2), 2.5 m (M3 and M4) and 2.0 m (M5), along the ~190 m depth
126 in the borehole. The borehole is located in a region where the typical vegetation is old cork
127 trees. This vegetation type has not changed in the last hundred years and the topography is
128 subdued, with small elevation variations of tens of meters in the nearest few kilometres. The
129 rock type in the area is hercynian age granite. Its thermophysical properties were measured in
130 four samples, collected in a quarry located in the same granitic body and 1.5 km eastwards of
131 the borehole. Thermal conductivity values of $2.8 \pm 0.2 \text{ W mK}^{-1}$ and thermal diffusivity values
132 of $1.3 \pm 0.1 \text{ m}^2 \text{ s}^{-1}$ were measured on polished surfaces of rock samples. Heat production was
133 calculated as $2 \pm 1 \text{ W m}^{-3}$ (Correia and Šafanda, 2001). The estimated heat flux density for the
134 borehole is 60 mW m^{-2} , which was confirmed as an *a posteriori* value of $58 \pm 13 \text{ mW m}^{-2}$
135 using the Functional Space Inversion method of Shen and Beck (1992).

136 The borehole temperature-depth profiles are herein compared to synthetic temperature
137 profiles (forward model), generated from both Lut2004 and annual mean near-surface

138 temperatures from two paleoclimate simulations, rather than applying the conventional
 139 procedure of inverting temperature logs to reconstruct ground surface temperatures (e.g.
 140 Correia and Šafanda, 2001). However, the uncertainties inherent to these inversion models
 141 (Hartmann and Rath, 2005), mostly due to errors in the estimation of subsurface parameters,
 142 are also present in these forward models. The profiles were generated following the
 143 methodology described by Beltrami et al. (2011), as explained below.

144 The temperature anomaly at depth z and time t , due to a step change in surface temperature T_0 ,
 145 is given by the solution of the one-dimensional heat diffusion equation (Carslaw and Jaeger,
 146 1959):

$$147 \quad T(z,t) = T_0 \operatorname{erfc}\left(\frac{z}{2\sqrt{kt}}\right), \quad (1)$$

148 where erfc is the complementary error function and k is the subsurface thermal diffusivity
 149 (Cermak and Rybach, 1982). It has a value of $1.3 \times 10^{-6} \text{ m}^2\text{s}^{-1}$, according to measurements on
 150 cut and polished surfaces of local rock samples (Correia and Šafanda, 2001). Generalizing
 151 this solution for a series of K step changes at the surface, the induced temperature anomalies
 152 at depth z are given by Mareschal and Beltrami (1992):

$$153 \quad T_i(z) = T_i(z) + \sum_{j=1}^K T_j \left[\operatorname{erfc}\left(\frac{z}{2\sqrt{kt_j}}\right) - \operatorname{erfc}\left(\frac{z}{2\sqrt{kt_{j-1}}}\right) \right], \quad (2)$$

154 where $T_i(z)$ is the initial temperature profile.

155

156 **2.3 Paleoclimate simulations**

157 The two paleoclimate simulations were carried out with the Global Circulation Model (GCM)
 158 – ECHO-G, and then dynamically downscaled with the Regional Climate Model (RCM) –
 159 MM5. ECHO-G combines the HOPE-G ocean model (Legutke and Voss, 1999) with the
 160 ECHAM4 atmospheric model (Roeckner et al., 1996). The regional model employs a limited
 161 area domain that spans completely the Iberian Peninsula with a spatial resolution of 30 km.
 162 Three reconstructed external forcings were used to consistently drive both models: solar
 163 variability, atmospheric greenhouse gas concentrations and radiative effects of stratospheric
 164 volcanic aerosols. The skill of the MM5/ECHO-G setup to reproduce the climate in the
 165 Iberian Peninsula has been previously evaluated by Gómez-Navarro et al. (2011), particularly

166 with respect to the ability of the regional model to reduce the warm bias and to correct the
167 winter variability over western Iberia in the GCM run. Two paleoclimate simulations (Sim1
168 and Sim2), only differing in their initial conditions, were used as a broad estimation of the
169 effect of internal variability (cf. Gómez-Navarro et al., 2012; González-Rouco et al., 2003;
170 Zorita et al., 2007; Zorita et al., 2005). Near-surface (2 m) temperatures for the period of
171 1600-1989 are extracted from these simulations. Their daily mean fields were bilinearly
172 interpolated from the original MM5 grid to the reconstructed temperature grid (0.5° latitude \times
173 0.5° longitude) and extracted for the above-defined Lisbon gridbox ($38.5\text{--}39.0^\circ\text{N}$, 8.0--
174 8.5°W). Annual (December–November) means were then computed from the raw 6-hourly
175 data.

176 In order to identify low-frequency variability and trends in the paleoclimate simulations, a
177 data-adaptive filtering, based on a singular spectral analysis (SSA), is applied (Ghil and
178 Vautard, 1991). SSA is based on the well-known principal component analysis, in which the
179 multiple dimensionality is achieved by including time-lagged replicas of the original time
180 series. The resulting principal components are thus linear combinations of different lags of
181 this series, which is equivalent to a time filtering with filter-coefficients that are related to the
182 eigenvectors of the lagged-covariance matrix. More formally, SSA corresponds to an
183 eigenvalue decomposition of a lagged-covariance matrix, with a Toeplitz structure, obtained
184 from the original time series of the paleoclimatic simulations. The rank, M , of this matrix is
185 the average of $(N/4\text{--}N/3)$, where N is the time series length (Plaut and Vautard, 1994). For the
186 paleoclimatic simulations $M=113$ ($N=390$). In this methodology, the original time series can
187 also be decomposed into a sum of M additive components and can be partially rebuilt using
188 only the leading ‘signal modes’, thus filtering out background noisy components (Elsner and
189 Tsonis, 1996; Vautard et al., 1992). In n -order SSA filtering, the leading n modes are used to
190 rebuild the original time series. The lower the number of retained modes, the stronger is the
191 time series smoothing. If all M modes are used, the original time series is fully recovered.

192 Under the assumption that the aforementioned external forcings used in the paleoclimate
193 simulations are mainly manifested by long-term temperature trends in western Iberia, as
194 suggested by Gómez-Navarro et al. (2012), similar trends of reconstructed and simulated
195 temperatures should be expected. As SSA enables isolating data-adaptive non-linear trends in
196 the time series (Ghil and Vautard, 1991), it can be used to correct discrepancies between long-
197 term trends of reconstructed and simulated temperature series. In the present study, this

198 approach was used to adjust the low-frequency variability in the reconstructed series to the
199 paleoclimate external forcings obtained from the simulations (adjustment of the Lut2004
200 reconstruction). Therefore, instead of developing a new reconstruction, an adjustment of the
201 already existing reconstruction was carried out herein (post-reconstruction adjustment).

202

203 **2.4 Instrumental data and indexed temperatures**

204 The consistency of the Lut2004 reconstruction with the corresponding instrumental series
205 (InstT) for the available period of 1901–1999, recorded at the Lisboa-Geofísico
206 meteorological station and supplied by the European Climate Assessment & Dataset project
207 (Klein Tank et al., 2002), was also assessed. It should be stressed that Lut2004 is heavily
208 dependent on InstT, as previously referred, and a high temporal correspondence between
209 these two time series is thereby expected. A transfer-function between InstT and Lut2004 was
210 determined by using a linear regression analysis. The resulting first-order regression
211 polynomial was applied so as to calibrate the Lut2004 reconstruction in the extended period
212 from 1600 onwards, thus correcting its location and scale parameters. Lastly, annual indexed
213 temperatures for southern Portugal over the pre-instrumental period of 1675–1715 (LMM),
214 developed by Alcoforado et al. (2000), were also analysed for consistency assessment.

215

216 **3. Results**

217 **3.1 Consistency with borehole measurements and paleoclimate simulations**

218 The consistency of the Lut2004 reconstruction with borehole temperature-depth profiles and
219 with paleoclimate simulations is assessed in this section. The five logs of borehole
220 measurements (M1, M2, M3, M4 and M5) are shown in Fig. 1a. Their corresponding inverse
221 geothermal gradients were estimated using linear regressions applied to the bottom 140–180
222 m data (Fig. 1b). Owing to the deposition of fine material at the bottom of the borehole, there
223 is locally a change in thermal conductivity at about 180 m. As the borehole was drilled in a
224 very homogeneous granite batholith, these changes are not due to changes in the geological
225 formation. In the present study, depths >180m are not used for gradient estimations. These
226 gradients approximately range from 46 to 48 m °C⁻¹ (ca. 0.021 °C m⁻¹). The corresponding
227 root-mean squared error (RMSE) of each estimated linear model is always <0.01°C (R-square
228 adjusted >99.9%), which means that the errors in the estimation of the geothermal gradients

229 have only minor impacts on the subsequent temperature-depth anomalies. The low borehole
230 depths require a word of caution, as some authors have indicated that 200 m of depth may be
231 too shallow for climate change assessments (Beltrami et al., 2011; Hamza et al., 2007;
232 Majorowicz et al., 1999). The Global Database of Borehole Temperatures and Climate
233 Reconstructions from the University of Michigan and the World Data Center for
234 Paleoclimatology indeed consider a 200 m depth as a minimum requirement for past climate
235 reconstruction (Pollack and Huang, 2000). Beltrami et al. (2011) also demonstrated that the
236 maximum depth of borehole profiles can have a large impact on temperature-depth anomalies.
237 Since no other geothermal-paleoclimatological observatory is available in Portugal, the
238 conclusions derived from these borehole profiles may be provisional.

239 The five temperature-depth anomaly profiles (M1–5), after removing their estimated
240 geothermal gradients, are reproduced in Fig. 2a. M1, M2, M3 and M4 show a more
241 pronounced near-surface warming than M5. Overall, these profiles suggest strong recent-past
242 warming trends in near-surface air temperatures.

243 The synthetic temperature-depth anomaly profiles, generated from the Lut2004 reconstruction
244 and from the two paleoclimate simulations, are also shown in Fig. 2a. The 11-year running
245 means of their anomalies over the period 1600–1989 are plotted in Fig. 2b. The chronograms
246 of the two simulations, as well as their individual profiles, are indeed very similar to the
247 corresponding ensemble mean chronograms and profiles (not shown). In fact, the correlation
248 coefficient between the 11-yr running means of the two simulations is as high as +0.82. This
249 is indicative of the large influence of external forcings in the long-term variability of
250 temperature. Conversely to the simulations, which exhibit a strong warming trend since the
251 1830s, Lut2004 only depicts a recent-past upward trend and a cooling trend during the
252 nineteenth century (Fig. 2b). Although the recent-past warming trend in Lut2004 is clearly
253 corroborated by InstT, the cooling trend is neither supported by simulations (Fig. 2b) nor by
254 any scientific evidence from previous studies. As a result, the synthetic temperature-depth
255 anomaly profile obtained from Lut2004 is clearly different from the profiles obtained from
256 the five borehole measurements and from the paleoclimate simulations (Fig.2a).

257 The discussion above hints at a remarkable agreement between the low-frequency variability
258 of near-surface temperature from two independent sources (borehole measurements and
259 paleoclimate simulations driven by reconstructed forcing). However, whereas the
260 paleoclimate simulations agree well with the borehole temperature-depth profiles, the

261 reconstructed temperature for Portugal (Lut2004) is not entirely consistent with the long-term
262 trends revealed by these new sources. In fact, its linear trend is nearly zero over the whole
263 period and there is no signature of cool/warm periods. This disagreement between simulations
264 and Lut2004 was already reported by Gómez-Navarro et al. (2011). As such, the low-
265 frequency variability of the Lut2004 reconstruction are herein adjusted to be more coherent
266 with the borehole data and simulations. Towards this aim, the ensemble mean temperature
267 from the two simulations was low-pass filtered by a 2-order SSA. The filtered series (SSA-
268 trend in Fig. 2b) highlights the signature of the external forcings on near-surface temperature
269 and was then added to the Lut2004 reconstruction. The resulting calibrated series (CalT =
270 Lut2004 + SSA-trend) is also shown in Fig. 2b.

271 The SSA-trend clearly shows a warming trend since the 1830s and a relatively cool period
272 during the LMM (1670–1730). This is also in line with previous studies on the impact of solar
273 activity on global temperatures (e.g. Eddy, 1983; Frenzel, 1994). The period from 1730 to
274 1800 recorded annual mean temperatures close to the baseline, being followed by an
275 anomalously cold period until the 1830s, which is associated with the Dalton Minimum, also
276 a period of low solar activity (Wagner and Zorita, 2005). The strong upward trend in CalT
277 from the 1830s onwards is now in clear agreement with the paleoclimate simulations and
278 InstT (in the twentieth century). The LMM (ca. 1670–1730) and Dalton minimum (ca. 1790–
279 1830) are also clearly depicted in CalT. Furthermore, the temperature-depth anomaly profile
280 from CalT is similar to the profiles from the five borehole measurements and paleoclimate
281 simulations (Fig. 2a). This represents an important validation of CalT.

282

283 **3.2 Consistency with instrumental data**

284 The consistency between InstT and CalT has been assessed by a linear regression in their
285 common period (1901–1989). The corresponding scatterplot shows that linear regression
286 provides a good fitting, with a correlation coefficient above 0.90 (Fig. 3), explaining about
287 82% of the total variance (R-square adjusted), and a RMSE of 0.22. According to the Fisher's
288 test, this least-squares linear regression model is statistically significant at a 99% confidence
289 level ($p < 0.01$). A bootstrap procedure with 10,000 resamples shows that the 95% confidence
290 interval for the correlation coefficient between InstT and CalT is [0.87, 0.93], supporting the
291 Fisher's test. Therefore, CalT clearly reproduces the observed temperature in Portugal in the
292 instrumental period (InstT). A 3-order polynomial fitting, with a robust regression using the

293 bisquare weighting method, provides a slightly better adjustment (R-square adjusted of 83%
294 and RMSE of 0.21), but its extrapolation for the lowest temperatures (outside the range of
295 values used in the model fitting, not shown) is not reliable and was discarded. The
296 corresponding linear regression polynomial is applied for a second-stage adjustment of
297 location and scale parameters in CalT. This allows expressing CalT in absolute temperature
298 values instead of anomalies (Fig. 4a). Additionally, taking into account the high coherency
299 between CalT and InstT, CalT was extended from 1989 to 1999 using InstT values. In order
300 to confirm long-term trends in CalT, the non-parametric progressive Mann-Kendall test is
301 applied (Sneyers, 1990, 1992). The forward and backward Kendall t parameters for CalT
302 jointly depict a warming trend from the 1830s onwards, being particularly noteworthy since
303 the 1930s (Fig.4b).

304 The uncertainties in the CalT series are a combination of the original uncertainties in the
305 Lut2004 dataset plus additional uncertainties related to the non-linear trend used in the
306 adjustment. The former are discussed in Luterbacher et al. (2004), but are only available for
307 the European mean reconstruction. Hence, it is not possible to have a local estimate of these
308 uncertainties. The latter can be estimated through the assessment of the consistence between
309 Sim1 and Sim2. For this purpose, the SSA filtering was applied separately to Sim1 and Sim2.
310 The mean absolute difference between the two non-linear trends obtained from Sim1 and
311 Sim2 provides a measure of the uncertainty related to the simulations. It has an approximate
312 value of 0.05°C. However, this number provides just a lower bound, since it does not
313 explicitly consider uncertainties related to the simulation itself, which are difficult to assess
314 due to the limited number of available simulations with similar characteristics.

315

316 **3.3 Consistency with precipitation indices**

317 In previous studies, temperature in southern Portugal was analysed during the LMM (1675–
318 1715) by Alcoforado et al. (2000), and during the eighteenth century by Taborda et al. (2004)
319 and Alcoforado et al. (2012). In these studies, research was based on documentary evidence,
320 such as diaries, ecclesiastical rogation ceremonies (*pro-pluvia* and *pro-serenitate*),
321 *Misericórdias* and municipal institutional sources, as well as on early instrumental data. From
322 this documentary evidence, basic data were transformed into indices on an ordinal scale,
323 following the methodology developed by Pfister (1995). Monthly temperatures were
324 originally indexed on a scale from 0 to ± 1 . Annual indices (December–November) can then

325 vary from 0 to ± 12 . The consistency between CalT and the corresponding annual indexed
326 temperatures is assessed by their respective scatterplots (Fig. 5). For a perfect agreement, the
327 documented temperature extremes (cold/hot years) should be reflected by coherent CalT
328 anomalies, i.e. all data pairs in the scatterplots should be either on top-right or bottom-left
329 quadrants (positively aligned series). There is an overall agreement between CalT and the
330 annual temperature index (>80% of all years are on top-right or bottom-left quadrants, with a
331 correlation coefficient of 0.76). Therefore, this agreement also provides a validation of CalT
332 for the period of 1675–1715. However, as the SSA-filtering does not significantly modify the
333 interannual variability within this relatively short time period (LMM), the aforementioned
334 agreement also applies between Lut2004 and the annual temperature index (not shown).

335

336 **4. Summary and conclusions**

337 The consistency of the reconstructed annual temperature series in Portugal (Lut2004) is
338 assessed by using five borehole temperature-depth profiles, synthetic temperature-depth
339 profiles generated from both the Lut2004 reconstruction and paleoclimate simulations,
340 instrumental data (InstT) and indexed temperatures during the LMM. While the paleoclimate
341 simulations agree well in the long-term variability with the borehole temperature-depth
342 profiles, the same does not apply to the Lut2004 reconstruction. In fact, the long-term trends
343 in Lut2004 are not fully consistent with borehole data and simulations. The late Maunder and
344 Dalton minima, clearly reflected in the paleoclimate simulations and well-documented in the
345 literature, in association with changes in solar activity (Eddy, 1983), are absent from the
346 Lut2004 reconstruction. Moreover, there is a cooling trend throughout the nineteenth century
347 that is not supported by previous studies. Therefore, the Lut2004 reconstruction was
348 calibrated by adjusting its low-frequency variability to the paleoclimatic simulations, also in
349 agreement with local borehole data. Documentary sources in Portugal during the LMM
350 (1675–1715) also show high agreement with CalT, thus providing an additional validation
351 over the LMM.

352 These results suggest some inconsistencies in the low-frequency variability of temperature in
353 Portugal between the Lut2004 reconstruction and borehole data or simulations. In effect, the
354 absence of clear long-term trends in Lut2004 is not coherent with the significant changes in
355 the radiative forcing throughout the last 400 years and the important role played by these
356 external forcings on temperature variability over western Iberia (Gómez-Navarro et al., 2012).

357 The frequent temporal gaps in the pre-instrumental records and the substantial lack of natural
358 proxies with clear climatic signals in Portugal (Alcoforado et al., 2012; Camuffo et al., 2010;
359 Luterbacher et al., 2006) may partially explain this limitation in the reproduction of the low-
360 frequency variability in the Lut2004 reconstruction. An important loss of low-frequency
361 variance caused by the method used in Lut2004 was also found by von Storch et al. (2009).
362 Nevertheless, a more detailed assessment of the causes for this shortcoming is out of the
363 scope of the present study, as it does not develop a new reconstruction for comparison, but
364 rather an adjustment of an existing reconstruction.

365 CalT adjusts the low-frequency variability in the Lut2004 reconstruction so as to be more
366 consistent with local borehole measurements and regional climate simulations. It can thus be
367 of foremost relevance in forthcoming research on climatic variability in Portugal. A reliable
368 representation of the low-frequency variability of temperature in Portugal, including its long-
369 term trends, is critical for understanding the role played by external vs. internal forcings on
370 the regional climate variability and change. Due to the relatively coarse spatial resolution of
371 data generated by state-of-the-art GCMs, they are not suitable for regional-scale assessments.
372 Since such scales are precisely the focus of this study, temperature series from two high-
373 resolution regional paleoclimatic simulations (Sim1 and Sim2) are employed instead of GCM
374 runs. These two simulations were documented and validated in previous studies.
375 Unfortunately, there are only two available simulations covering Portugal with such high-
376 resolution characteristics. Hence, it is not possible to increase the ensemble size of model
377 simulations, though it would be very useful for uncertainty assessments. In forthcoming
378 research, new regional paleoclimatic simulations over Portugal, also using different models,
379 should be used to enhance the robustness and evaluate the significance of the current
380 adjustment.

381

382 *Acknowledgements.* This study was carried out within the framework of the project
383 ‘Reconstruction and model simulations of past climate in Portugal, using documentary and
384 early instrumental sources – Klimhist’ and was supported by national funds from FCT -
385 Portuguese Foundation for Science and Technology [PTDC/AAC-CLI/119078/2010] and
386 [UID/AGR/04033/2013].

387

388 **References**

- 389 Ahmed, M., Anchukaitis, K. J., Asrat, A., Borgaonkar, H. P., Braidia, M., Buckley, B. M.,
390 Buntgen, U., Chase, B. M., Christie, D. A., Cook, E. R., Curran, M. A. J., Diaz, H. F., Esper,
391 J., Fan, Z. X., Gaire, N. P., Ge, Q. S., Gergis, J., Gonzalez-Rouco, J. F., Goosse, H., Grab, S.
392 W., Graham, N., Graham, R., Grosjean, M., Hanhijarvi, S. T., Kaufman, D. S., Kiefer, T.,
393 Kimura, K., Korhola, A. A., Krusic, P. J., Lara, A., Lezine, A. M., Ljungqvist, F. C., Lorrey,
394 A. M., Luterbacher, J., Masson-Delmotte, V., McCarroll, D., McConnell, J. R., McKay, N. P.,
395 Morales, M. S., Moy, A. D., Mulvaney, R., Mundo, I. A., Nakatsuka, T., Nash, D. J.,
396 Neukom, R., Nicholson, S. E., Oerter, H., Palmer, J. G., Phipps, S. J., Prieto, M. R., Rivera,
397 A., Sano, M., Severi, M., Shanahan, T. M., Shao, X. M., Shi, F., Sigl, M., Smerdon, J. E.,
398 Solomina, O. N., Steig, E. J., Stenni, B., Thamban, M., Trouet, V., Turney, C. S. M., Umer,
399 M., van Ommen, T., Verschuren, D., Viau, A. E., Villalba, R., Vinther, B. M., von Gunten,
400 L., Wagner, S., Wahl, E. R., Wanner, H., Werner, J. P., White, J. W. C., Yasue, K., Zorita, E.,
401 and Consortium, P. k.: Continental-scale temperature variability during the past two
402 millennia, *Nat. Geosci.*, 6, 339-346, doi:10.1038/Ngeo1797, 2013.
- 403 Alcoforado, M. J., Nunes, M. F., Garcia, J. C., and Taborda, J. P.: Temperature and
404 precipitation reconstruction in southern Portugal during the late Maunder Minimum (AD
405 1675–1715), *Holocene*, 10, 333–340, 2000.
- 406 Alcoforado, M. J., Vaquero, J. M., Trigo, R. M., and Taborda, J. P.: Early Portuguese
407 meteorological measurements (18th century), *Clim. Past*, 8, 353–371, doi:10.5194/cp-8-353-
408 2012, 2012.
- 409 Beltrami, H. and Bourlon, E.: Ground warming patterns in the Northern Hemisphere during
410 the last five centuries, *Earth Planet. Sc. Lett.*, 227, 169–177, 2004.
- 411 Beltrami, H. and Mareschal, J.-C.: Resolution of ground temperature histories inverted from
412 borehole temperature data, *Global Planet. Change*, 11, 57–70, 1995.
- 413 Beltrami, H., González-Rouco, J. F., and Stevens, M. B.: Subsurface temperatures during the
414 last millennium: model and observation, *Geophys. Res. Lett.*, 33, L09705,
415 doi:10.1029/2006GL026050, 2006.
- 416 Beltrami, H., Smerdon, J. E., Matharoo, G. S., and Nickerson, N.: Impact of maximum
417 borehole depths on inverted temperature histories in borehole paleoclimatology, *Clim. Past*, 7,
418 745–756, doi:10.5194/cp-7-745-2011, 2011.
- 419 Bodri, L. and Čermák, V.: Reconstruction of remote climate changes from borehole
420 temperatures, *Global Planet. Change*, 15, 47-57, doi:10.1016/S0921-8181(97)00004-0, 1997.
- 421 Brázdil, R., Dobrovolný, P., Luterbacher, J., Moberg, A., Pfister, C., Wheeler, D., and Zorita,
422 E.: European climate of the past 500 years: new challenges for historical climatology,
423 *Climatic Change*, 101, 7-40, doi:10.1007/s10584-009-9783-z, 2010.
- 424 Brázdil, R., Pfister, C., Wanner, H., Storch, H., and Luterbacher, J.: Historical Climatology In
425 Europe – The State Of The Art, *Climatic Change*, 70, 363-430, doi:10.1007/s10584-005-
426 5924-1, 2005.

- 427 Camuffo, D., Bertolin, C., Barriendos, M., Dominguez-Castro, F., Cocheo, C., Enzi, S.,
428 Sghedoni, M., Valle, A., Garnier, E., Alcoforado, M. J., Xoplaki, E., Luterbacher, J., Diodato,
429 N., Maugeri, M., Nunes, M. F., and Rodriguez, R.: 500-year temperature reconstruction in the
430 Mediterranean Basin by means of documentary data and instrumental observations, *Climatic*
431 *Change*, 101, 169-199, doi:10.1007/s10584-010-9815-8, 2010.
- 432 Camuffo, D., Bertolin, C., Diodato, N., Cocheo, C., Barriendos, M., Dominguez-Castro, F.,
433 Garnier, E., Alcoforado, M. J., and Nunes, M. F.: Western Mediterranean precipitation over
434 the last 300 years from instrumental observations, *Climatic Change*, 117, 85-101,
435 doi:10.1007/s10584-012-0539-9, 2013.
- 436 Carslaw, H. S. and Jaeger, J. C.: *Conduction of Heat in Solids*, Oxford Univ. Press, New
437 York, 1959.
- 438 Cermak, V. and Rybach, L.: Thermal conductivity and specific heat of minerals and rocks. In:
439 Subvolume A, Angenheister, G. (Ed.), *Landolt-Börnstein - Group V Geophysics*, Springer
440 Berlin Heidelberg, 341–343, 1982.
- 441 Chouinard, C. and Mareschal, J. C.: Selection of borehole temperature depth profiles for
442 regional climate reconstructions, *Clim. Past*, 3, 297-313, doi:10.5194/cp-3-297-2007, 2007.
- 443 Correia, A. and Šafanda, J.: Ground surface temperature history at a single site in southern
444 Portugal reconstructed from borehole temperatures, *Global Planet. Change*, 29, 155-165,
445 doi:10.1016/S0921-8181(01)00087-X, 2001.
- 446 Correia, A. and Šafanda, J.: Preliminary ground surface temperature history in mainland
447 Portugal reconstructed from borehole temperature logs, *Tectonophysics*, 306, 269-275,
448 doi:10.1016/S0040-1951(99)00060-8, 1999.
- 449 Eddy, J. A.: The Maunder Minimum - a Reappraisal, *Sol. Phys.*, 89, 195-207,
450 doi:10.1007/Bf00211962, 1983.
- 451 Elsner, J. B. and Tsonis, A. A.: *Singular spectrum analysis: a new tool in time series analysis*,
452 Plenum Press, New York; London, 1996.
- 453 Frenzel, B.: *Climatic Trends and anomalies in Europe 1675-1715. High resolution spatio-*
454 *temporal reconstructions from direct meteorological observations and proxy data. Methods*
455 *and Results*, Gustav Fisher Verlag. Stuttgart, Jena and New York, 1994.
- 456 Ghil, M. and Vautard, R.: Interdecadal Oscillations and the Warming Trend in Global
457 Temperature Time-Series, *Nature*, 350, 324-327, doi:10.1038/350324a0, 1991.
- 458 Gómez-Navarro, J. J., Montavez, J. P., Jerez, S., Jimenez-Guerrero, P., Lorente-Plazas, R.,
459 Gonzalez-Rouco, J. F., and Zorita, E.: A regional climate simulation over the Iberian
460 Peninsula for the last millennium, *Clim. Past*, 7, 451-472, doi:10.5194/cp-7-451-2011, 2011.
- 461 Gómez-Navarro, J. J., Montávez, J. P., Jiménez-Guerrero, P., Jerez, S., Lorente-Plazas, R.,
462 González-Rouco, J. F., and Zorita, E.: Internal and external variability in regional simulations
463 of the Iberian Peninsula climate over the last millennium, *Clim. Past*, 8, 25-36,
464 doi:10.5194/cp-8-25-2012, 2012.

- 465 González-Rouco, F., von Storch, H., and Zorita, E.: Deep soil temperature as proxy for
466 surface air-temperature in a coupled model simulation of the last thousand years, *Geophys.*
467 *Res. Lett.*, 30, 2116, doi:10.1029/2003GL018264, 2003.
- 468 González-Rouco, J. F., Beltrami, H., Zorita, E., and Stevens, M. B.: Borehole climatology: a
469 discussion based on contributions from climate modeling, *Clim. Past*, 5, 97-127,
470 doi:10.5194/cp-5-97-2009, 2009.
- 471 González-Rouco, J. F., Beltrami, H., Zorita, E., and von Storch, H.: Simulation and inversion
472 of borehole temperature profiles in surrogate climates: Spatial distribution and surface
473 coupling, *Geophys. Res. Lett.*, 33, L01703, doi:10.1029/2005GL024693, 2006.
- 474 Gouirand, I., Moberg, A., and Zorita, E.: Climate variability in Scandinavia for the past
475 millennium simulated by an atmosphere-ocean general circulation model, *Tellus A*, 59, 30-49,
476 doi:10.1111/j.1600-0870.2006.00207.x, 2007.
- 477 Hamza, V. M., Cavalcanti, A. S. B., and Benyosef, L. C. C.: Surface thermal perturbations of
478 the recent past at low latitudes - inferences based on borehole temperature data from Eastern
479 Brazil, *Clim. Past*, 3, 513-526, 2007.
- 480 Harris, R. N. and Chapman, D. S.: Geothermics and climate change: 1. Analysis of borehole
481 temperatures with emphasis on resolving power, *J. Geophys. Res.-Sol. Ea.*, 103, 7363-7370,
482 doi:10.1029/97JB03297, 1998.
- 483 Harris, R. N. and Gosnold, W. D.: Comparisons of borehole temperature–depth profiles and
484 surface air temperatures in the northern plains of the USA, *Geophys. J. Int.*, 138, 541-548,
485 doi:10.1046/j.1365-246X.1999.00884.x, 1999.
- 486 Hartmann, A. and Rath, V.: Uncertainties and shortcomings of ground surface temperature
487 histories derived from inversion of temperature logs, *J. Geophys. Eng.*, 2, 299,
488 doi:10.1088/1742-2132/2/4/S02, 2005.
- 489 IPCC: Climate Change 2013: The Physical Science Basis. Contribution of Working Group I
490 to the Fifth Assessment Report of the Intergovernmental Panel on Climate Change [Stocker,
491 T.F., D. Qin, G.-K. Plattner, M. Tignor, S.K. Allen, J. Boschung, A. Nauels, Y. Xia, V. Bex
492 and P.M. Midgley (eds.)]. Cambridge University Press, Cambridge, United Kingdom and
493 New York, NY, USA, 1535 pp., 2013.
- 494 Jones, P. D., Briffa, K. R., Osborn, T. J., Lough, J. M., van Ommen, T. D., Vinther, B. M.,
495 Luterbacher, J., Wahl, E. R., Zwiers, F. W., Mann, M. E., Schmidt, G. A., Ammann, C. M.,
496 Buckley, B. M., Cobb, K. M., Esper, J., Goosse, H., Graham, N., Jansen, E., Kiefer, T., Kull,
497 C., Kuttel, M., Mosley-Thompson, E., Overpeck, J. T., Riedwyl, N., Schulz, M., Tudhope, A.
498 W., Villalba, R., Wanner, H., Wolff, E., and Xoplaki, E.: High-resolution palaeoclimatology
499 of the last millennium: a review of current status and future prospects, *Holocene*, 19, 3-49,
500 doi:10.1177/0959683608098952, 2009.
- 501 Klein Tank, A. M. G., Wijngaard, J. B., Können, G. P., Böhm, R., Demarée, G., Gocheva, A.,
502 Mileta, M., Pashiardis, S., Hejkrlik, L., Kern-Hansen, C., Heino, R., Bessemoulin, P., Müller-
503 Westermeier, G., Tzanakou, M., Szalai, S., Pálsdóttir, T., Fitzgerald, D., Rubin, S., Capaldo,
504 M., Maugeri, M., Leitass, A., Bukantis, A., Aberfeld, R., van Engelen, A. F. V., Forland, E.,
505 Miletus, M., Coelho, F., Mares, C., Razuvaev, V., Nieplova, E., Cegnar, T., Antonio López, J.,

- 506 Dahlström, B., Moberg, A., Kirchhofer, W., Ceylan, A., Pachaliuk, O., Alexander, L. V., and
507 Petrovic, P.: Daily dataset of 20th-century surface air temperature and precipitation series for
508 the European Climate Assessment, *Int. J. Climatol.*, 22, 1441-1453, doi:10.1002/joc.773,
509 2002.
- 510 Legutke, S. and Voss, R.: The Hamburg atmosphere–ocean coupled circulation model
511 ECHOG, Germany DKRZ Tech. Rep. 18, Dtsch. Klimarechenzentrum, Hamburg, 1999.
- 512 Li, B., Nychka, D. W., and Ammann, C. M.: The Value of Multiproxy Reconstruction of Past
513 Climate, *J. Am. Stat. Assoc.*, 105, 883-895, doi:10.1198/jasa.2010.ap09379, 2010.
- 514 Luterbacher, J., Dietrich, D., Xoplaki, E., Grosjean, M., and Wanner, H.: European seasonal
515 and annual temperature variability, trends, and extremes since 1500, *Science*, 303, 1499-1503,
516 doi:10.1126/science.1093877, 2004.
- 517 Luterbacher, J., Xoplaki, E., Casty, C., Wanner, H., Pauling, A., Küttel, M., Rutishauser, T.,
518 Brönnimann, S., Fischer, E., Fleitmann, D., Gonzalez-Rouco, F. J., García-Herrera, R.,
519 Barriendos, M., Rodrigo, F., Gonzalez-Hidalgo, J. C., Saz, M. A., Gimeno, L., Ribera, P.,
520 Brunet, M., Paeth, H., Rimbu, N., Felis, T., Jacobeit, J., Dünkeloh, A., Zorita, E., Guiot, J.,
521 Türkeş, M., Alcoforado, M. J., Trigo, R., Wheeler, D., Tett, S., Mann, M. E., Touchan, R.,
522 Shindell, D. T., Silenzi, S., Montagna, P., Camuffo, D., Mariotti, A., Nanni, T., Brunetti, M.,
523 Maugeri, M., Zerefos, C., Zolt, S. D., Lionello, P., Nunes, M. F., Rath, V., Beltrami, H.,
524 Garnier, E., and Ladurie, E. L. R.: Chapter 1 Mediterranean climate variability over the last
525 centuries: A review. In: *Mediterranean climate variability*, P. Lionello, Malanotte-Rizzoli, P.,
526 and Boscolo, R. (Eds.), Elsevier, 2006.
- 527 Majorowicz, J. A., Šafanda, J., Harris, R. N., and Skinner, W. R.: Large ground surface
528 temperature changes of the last three centuries inferred from borehole temperatures in the
529 Southern Canadian Prairies, Saskatchewan, *Global and Planet. Change*, 20, 227-241,
530 doi:10.1016/S0921-8181(99)00016-8, 1999.
- 531 Mareschal, J. C. and Beltrami, H.: Evidence for recent warming from perturbed geothermal
532 gradients: examples from eastern Canada, *Clim. Dynam.*, 6, 135-143,
533 doi:10.1007/BF00193525, 1992.
- 534 New, M., Hulme, M., and Jones, P.: Representing twentieth-century space-time climate
535 variability. Part II: Development of 1901-96 monthly grids of terrestrial surface climate, *J.*
536 *Climate*, 13, 2217-2238, 2000.
- 537 Nielsen, S. B. and Beck, A. E.: Heat-Flow Density Values and Paleoclimate Determined from
538 Stochastic Inversion of 4 Temperature Depth Profiles from the Superior Province of the
539 Canadian Shield, *Tectonophysics*, 164, 345-359, 1989.
- 540 Pfister, C.: Monthly temperature and precipitation in central Europe from 1525-1979:
541 quantifying documentary evidence on weather and its effects. In: *Climate since A.D. 1500*,
542 Bradley, R. S. and Jones, P. D. (Eds.), Routledge, London, 1995.
- 543 Plaut, G. and Vautard, R.: Spells of Low-Frequency Oscillations and Weather Regimes in the
544 Northern-Hemisphere, *J. Atmos. Sci.*, 51, 210-236, 1994.

- 545 Pollack, H. N. and Huang, S. P.: Climate reconstruction from subsurface temperatures, *Annu.*
546 *Rev. Earth. Pl. Sc.*, 28, 339-365, doi:10.1146/annurev.earth.28.1.339, 2000.
- 547 Pollack, H. N., Huang, S. P., and Smerdon, J. E.: Five centuries of climate change in
548 Australia: the view from underground, *J. Quaternary Sci.*, 21, 701-706, doi:10.1002/Jqs.1060,
549 2006.
- 550 Roeckner, E., Arpe, K., Bengtsson, L., Christoph, M., Claussen, M., Dumenil, L., Esch, M.,
551 Giorgetta, M., Schlese, U., and Schulzweida, U.: The atmospheric general circulation model
552 ECHAM4: model description and simulation of present-day climate, Max-Planck-Institut für
553 Meteorologie, Hamburg, Germany Tech. Rep., 218, 1996.
- 554 Šafanda, J., Rajver, D., Correia, A., and Dedecek, P.: Repeated temperature logs from Czech,
555 Slovenian and Portuguese borehole climate observatories, *Clim. Past*, 3, 453-462,
556 doi:10.5194/cp-3-453-2007, 2007.
- 557 Shen, P. Y. and Beck, A. E.: Paleoclimate Change and Heat-Flow Density Inferred from
558 Temperature Data in the Superior Province of the Canadian Shield, *Global and Planetary*
559 *Change*, 98, 143-165, 1992.
- 560 Sneyers, R.: *On the Statistical Analysis of Series of Observations*, Secretariat of the World
561 Meteorological Organization, Geneva, Switzerland, 1990.
- 562 Sneyers, R.: Use and measure of statistical methods for detection of climatic change, in:
563 Climate Change Detection Project. Report on the Informal Planning Meeting on Statistical
564 Procedures for Climate Change Detection, WCDMP, 20, 176–181, Geneva, Switzerland,
565 1992.
- 566 Stevens, M. B., González-Rouco, J. F., and Beltrami, H.: North American climate of the last
567 millennium: Underground temperatures and model comparison, *J. Geophys. Res.-Earth*, 113,
568 F01008, doi:10.1029/2006JF000705, 2008.
- 569 Taborda, J. P., Alcoforado, M. J., and Garcia, J. C.: Climate in southern Portugal in the 18th
570 century. Reconstruction based on documentary and early instrumental sources (in
571 Portuguese, with extended English summary), University of Lisbon, Geo-Ecologia, 2, CEG,
572 Lisboa, ISBN: 972-636-144-3, 2004.
573 http://clima.ul.pt/images/pdf/pub/b_mja_2004_climasulportugal.pdf
- 574 Vautard, R., Yiou, P., and Ghil, M.: Singular-Spectrum Analysis - a Toolkit for Short, Noisy
575 Chaotic Signals, *Physica D*, 58, 95-126, 1992.
- 576 von Storch, H., Zorita, E., and Gonzalez-Rouco, F.: Assessment of three temperature
577 reconstruction methods in the virtual reality of a climate simulation, *Int. J. Earth Sci.*, 98, 67-
578 82, doi:10.1007/s00531-008-0349-5, 2009.
- 579 Wagner, S. and Zorita, E.: The influence of volcanic, solar and the Dalton Minimum (1790-
580 1830): CO₂ forcing on the temperatures in a model study, *Clim. Dyn.*, 25, 205-218,
581 doi:10.1007/s00382-005-0029-0, 2005.

- 582 Xoplaki, E., Luterbacher, J., Paeth, H., Dietrich, D., Steiner, N., Grosjean, M., and Wanner,
583 H.: European spring and autumn temperature variability and change of extremes over the last
584 half millennium, *Geophys. Res. Lett.*, 32, L15713, doi:10.1029/2005GL023424, 2005.
- 585 Zorita, E., Gonzalez-Rouco, F., and von Storch, H.: Comments on “Testing the Fidelity of
586 Methods Used in Proxy-Based Reconstructions of Past Climate”, *J. Climate*, 20, 3693-3698,
587 doi:10.1175/JCLI4171.1, 2007.
- 588 Zorita, E., González-Rouco, J. F., von Storch, H., Montávez, J. P., and Valero, F.: Natural and
589 anthropogenic modes of surface temperature variations in the last thousand years, *Geophys.*
590 *Res. Lett.*, 32, L08707, doi:10.1029/2004GL021563, 2005.
- 591

592 **Figure Captions**

593 **Fig. 1.** (a) Borehole temperature logs (temperature vs. depth) for: M1, M2, M3, M4 and M5 from the Évora
594 observatory (cf. legends). (b) The same as on (a), but only for the bottom 140–180 m data. The outlined
595 equations of the respective regression lines (omitted) represent the corresponding estimated geothermal gradients
596 (slope of the linear regression line).

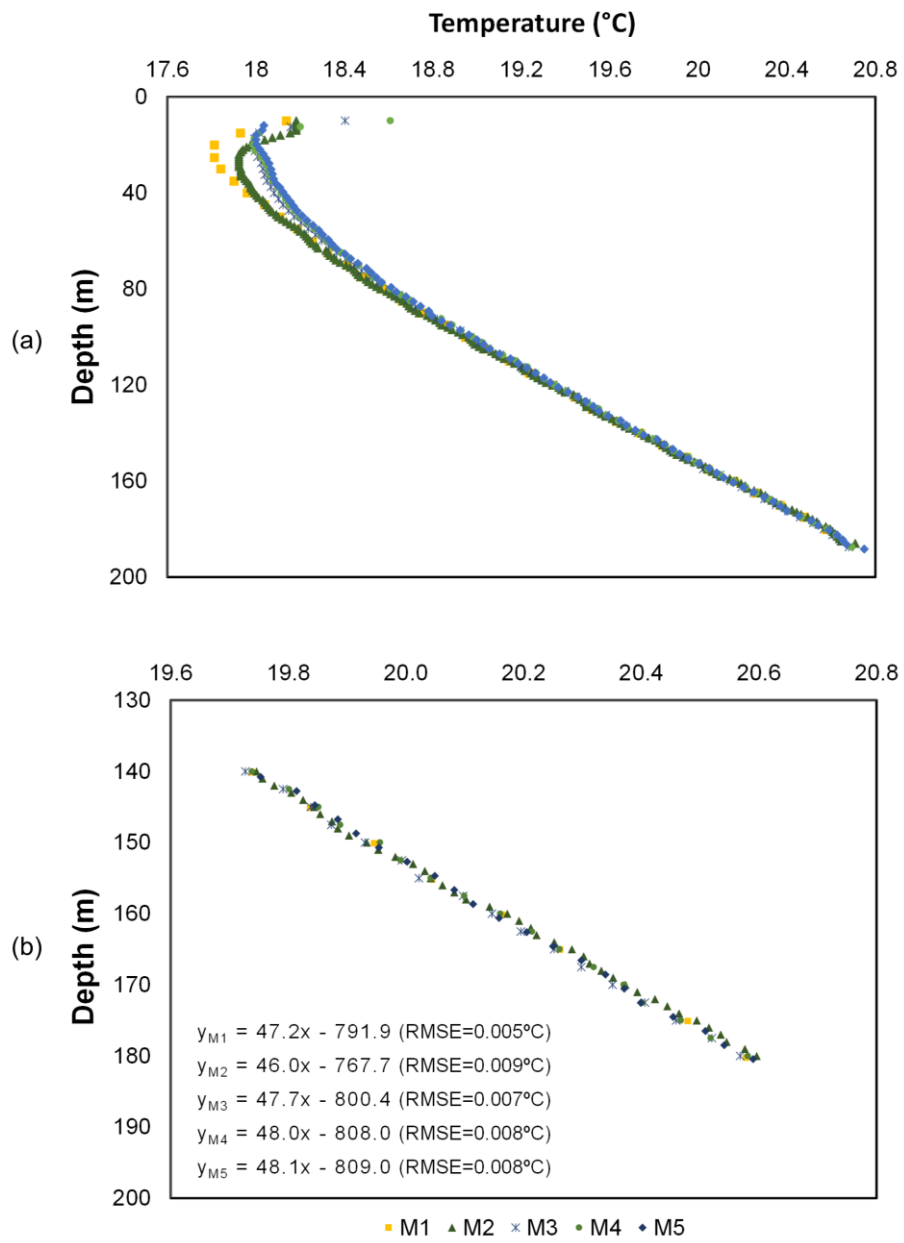
597 **Fig. 2.** (a) Temperature-depth anomaly profiles for: M1, M2, M3, M4 and M5, with respect to the estimated
598 geothermal gradients in Fig. 1b, along with the synthetic profiles generated from: Lut2004 – reconstructed
599 temperature; CalT – calibrated temperature; and Sim1/Sim2 – paleoclimate simulations, retrieved for a gridbox
600 near Lisbon, Portugal (cf. legends). (b) Chronograms of the 11-yr running mean anomalies of Lut2004, CalT and
601 Sim1/Sim2 for the period of 1600–1989. The SSA filtered ensemble mean temperature from the two simulations
602 (SSA-trend) is also displayed. The 11-yr running means of InstT (instrumental annual mean temperature)
603 anomalies are depicted for the period of 1901–1999, along with the respective linear trend. Note that anomalies
604 in each series are with respect to their common period (1901–1989).
605

606 **Fig. 3.** Scatterplot between InstT and CalT anomalies over their common period (1901–1989). The
607 corresponding regression line, calibration equation and R-squared measure (determination coefficient) are also
608 pointed out.

609 **Fig. 4.** Chronogram of: (a) CalT – calibrated annual mean temperature – in the period of 1600–1999 and InstT in
610 the period of 1901–1999. Estimated errors are grey shaded, with a mean error of 0.05°C (b) Forward – $u(t)$ – and
611 backward – $u'(t)$ – series of the normalised Kendall t parameter from the progressive Mann-Kendall analysis of
612 CalT. 95% confidence interval for the no trend hypothesis in grey shading.
613

614 **Fig. 5.** Scatterplot of CalT in the period of 1675–1715 as a function of the annual temperature indices. Light
615 (dark) grey circles represent cold (hot) years from documentary evidence. Circles with black edges indicate
616 agreement between the two datasets. Years with '0' index are omitted for the sake of readability of the plot. The
617 horizontal line corresponds to CalT mean. Some labels are omitted for the sake of clarity.

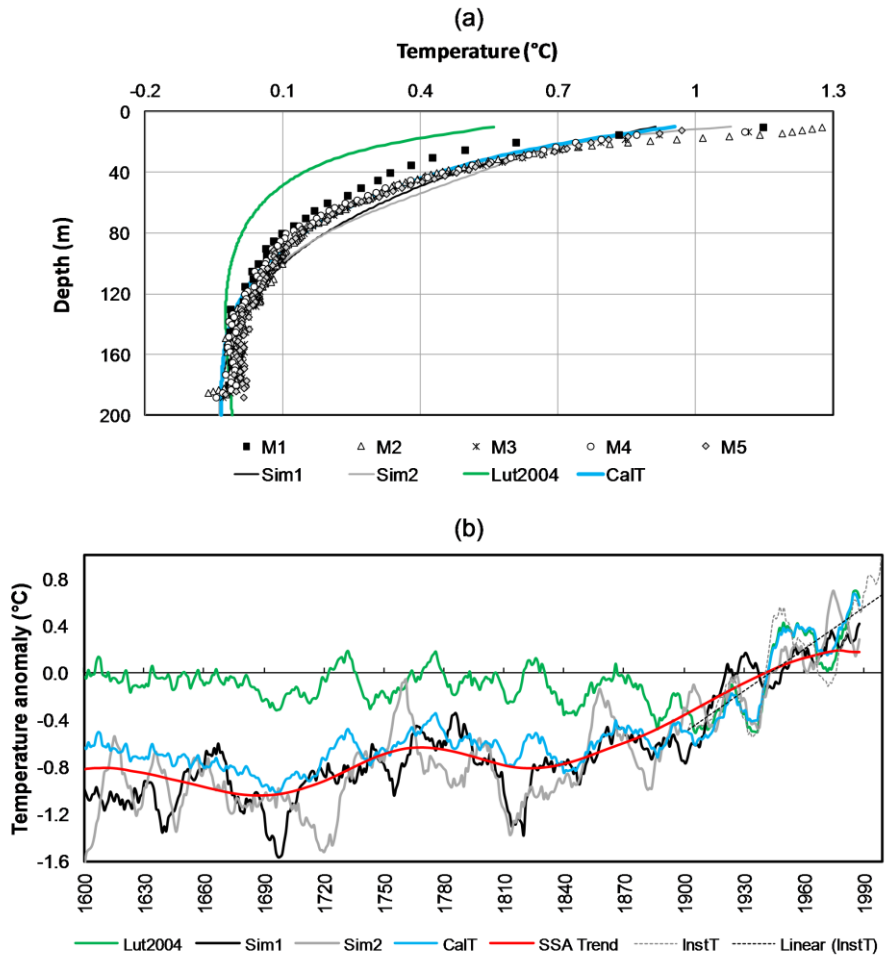
618



619
620
621

Fig. 1

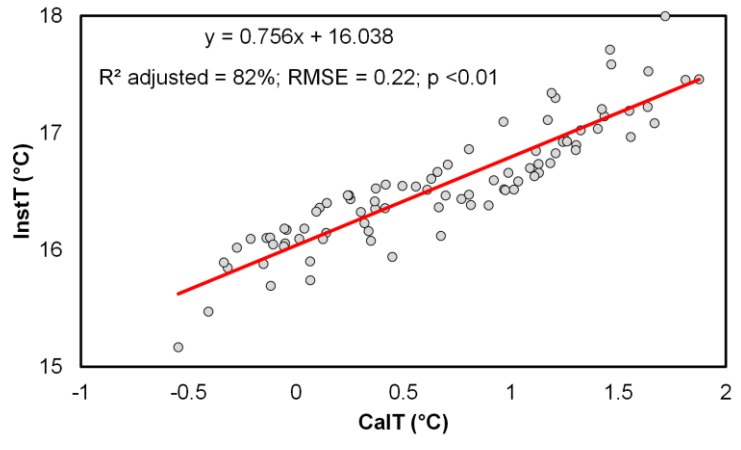
622



623
624
625

Fig. 2

626



627
628
629

Fig. 3

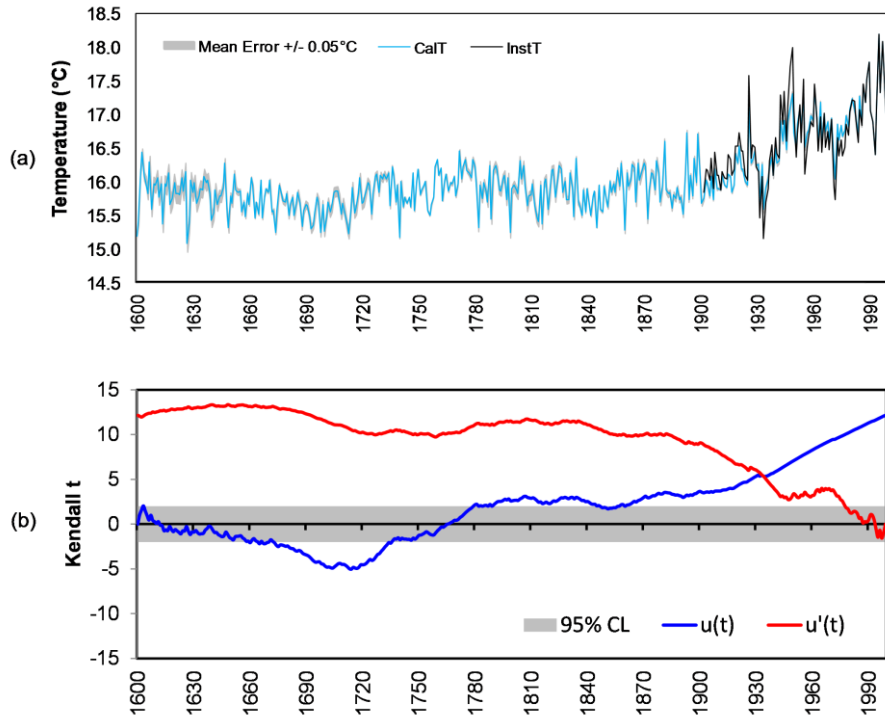
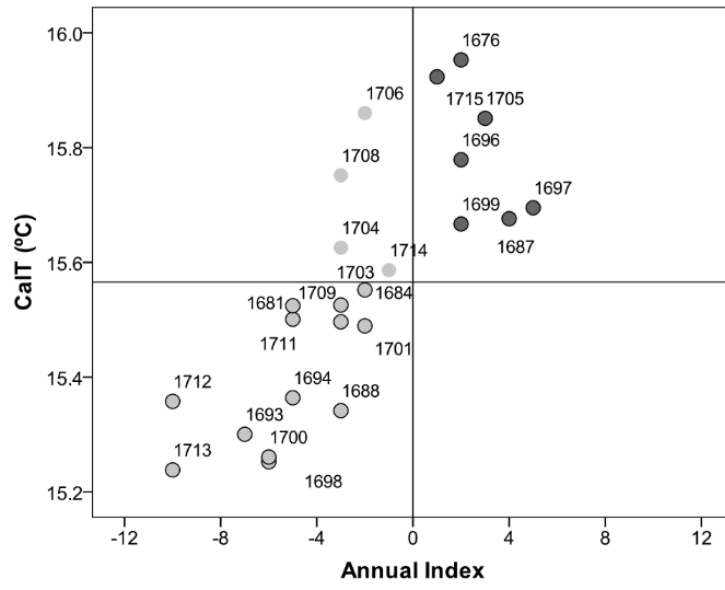


Fig. 4

631
632
633
634

635



636
637
638

Fig. 5